Population Redistribution Among Multiple Electronic States of Molecular Nitrogen Ions in Strong Laser Fields

Jinping Yao,[1] Shicheng Jiang,[2] Wei Chu,[1] Bin Zeng,[1] Chengyin Wu,[3,4,*] Ruifeng Lu,[2,5,†] Ziting Li,[1,6] Hongqiang Xie,[1,7] Guihua Li,[1] Chao Yu,[2] Zhanshan Wang,[6] Hongbing Jiang,[3] Qihuang Gong,[3,4] and Ya Cheng[1,§]

[1]*State Key Laboratory of High Field Laser Physics, Shanghai Institute of Optics and Fine Mechanics, Chinese Academy of Sciences, Shanghai 201800, China*

[2]*Department of Applied Physics, Nanjing University of Science and Technology, Nanjing 210094, China*

[3]*State Key Laboratory for Mesoscopic Physics, Department of Physics, Peking University, Beijing 100871, China*

[4]*Collaborative Innovation Center of Quantum Matter, Beijing 100871, China*

[5]*State Key Laboratory of Molecular Reaction Dynamics, Dalian Institute of Chemical Physics, Chinese Academy of Sciences, Dalian 116023, China*

[6]*School of Physics Science and Engineering, Tongji University, Shanghai 200092, China*

[7]*University of Chinese Academy of Sciences, Beijing 100049, China*

(Received 10 June 2015; published 8 April 2016)

We carry out a combined theoretical and experimental investigation on the population distributions in the ground and excited states of tunnel-ionized nitrogen molecules at various driver wavelengths in the near- and midinfrared range. Our results reveal that efficient couplings (i.e., population exchanges) between the ground $N_2^+(X^2\Sigma_g^+)$ state and the excited $N_2^+(A^2\Pi_u)$ and $N_2^+(B^2\Sigma_u^+)$ states occur in strong laser fields. The couplings result in a population inversion between the $N_2^+(X^2\Sigma_g^+)$ and $N_2^+(B^2\Sigma_u^+)$ states at wavelengths near 800 nm, which is verified by our experimental observation of the amplification of a seed at ~391 nm. The result provides insight into the mechanism of free-space nitrogen ion lasers generated in remote air with strong femtosecond laser pulses.

DOI: 10.1103/PhysRevLett.116.143007

Tunnel ionization is a fundamental process for molecules in intense laser fields when the Keldysh parameter is less than unity [1]. It naturally launches an attosecond electron bunch with kinetic energy up to the ~100 eV level, enabling probing molecular dynamics with subfemtosecond, sub-Ångström spatiotemporal resolution based on either electron-recollision-induced dissociation [2–4] or laser-induced electron diffraction [5,6]. In addition, the tunnel ionization rate is also highly sensitive to the ionization potentials and orbital geometries of molecules, providing new opportunities for imaging molecular orbitals [7,8]. Recently, it has been further reported that strong laser fields can simultaneously induce tunnel ionizations from several molecular orbitals because of the multielectron effect and the close ionization potentials of the outermost and a few lower-lying orbitals [9–15]. A direct consequence of the multiorbital ionization is that the molecular ions can be populated in not only the ground but also the excited electronic states. As a commonly accepted assumption, the molecular ions in the excited electronic states are generated through the tunnel ionization from the lower-lying orbitals, with their populations being determined by the corresponding ionization probabilities.

Because molecular ions in the excited states can decay to the ground state by spontaneous fluorescence emission, fluorescence spectroscopy has been employed to identify the electronic states of the tunnel-ionized molecules and to determine their population distributions, which can be used to image the lower-lying molecular orbitals [13,15]. Owing to their higher ionization potentials, the exponential suppression of the ionization probabilities from the lower-lying orbitals suggests that the populations in the excited states should be much less than those in the ground state. Thus, it comes as a major surprise to observe a population inversion between $N_2^+(B^2\Sigma_u^+)$ and $N_2^+(X^2\Sigma_g^+)$ states when nitrogen molecules are subject to strong femtosecond laser pulses at a 800-nm wavelength [16]. The implication of the novel phenomenon on remote sensing applications has been widely recognized because it provides an ultrafast, intense free-space laser source in remote air [16–21]. However, the mechanism responsible for the population inversion is still far from being understood. One may argue that the population inversion might be realized by other ionization or excitation channels, such as electron-recollision-induced excitation [2–4], the nonadiabatic multielectron effect [22], and electron correlation during ionization [23]. Indeed, these channels can promote the population of excited molecular ions, but their contributions are insufficient to produce the population inversion observed for nitrogen molecules in strong femtosecond laser pulses at a 800-nm wavelength. In this Letter, we present a combined theoretical and experimental investigation on the population dynamics of the tunnel-ionized nitrogen molecules at the ground and excited states. Our results reveal that efficient

couplings between the ground $N_2^+(X^2\Sigma_g^+)$ and the excited $N_2^+(A^2\Pi_u)$ and $N_2^+(B^2\Sigma_u^+)$ states enable the generation of the population inversion between $N_2^+(X^2\Sigma_g^+)$ and $N_2^+(B^2\Sigma_u^+)$ states at pump wavelengths near 800 nm, which explains the experimental observations of the amplification of an external seed at ~391 nm and clarifies the mechanism of free-space nitrogen ion lasers generated in remote air with strong femtosecond laser pulses.

The experiments were carried out using a Ti:sapphire laser (Legend Elite-Duo, Coherent Inc.) and an optical parametric amplifier (OPA) (HE-TOPAS, Light Conversion Ltd.). The femtosecond laser pulses (1 kHz, 800 nm, ~40 fs) from the Ti:sapphire laser were first split into two beams. One beam with a pulse energy of ~6.5 mJ was injected into the OPA to generate wavelength-tunable midinfrared laser pulses in the spectral range from 1200 to 2400 nm, enabling us to perform the experiment at either 800 nm or midinfrared pump wavelengths. The pulse energies at all wavelengths were chosen to be ~800 μJ. The other beam with a pulse energy of 300 μJ was frequency doubled by a $\beta - BaB_2O_4$ (BBO) crystal; it then served as an external seed. To obtain the strongest amplification at the ~391-nm wavelength with the seed pulses, we carefully tuned the BBO crystal to slightly adjust the central wavelength of the seed pulse. The time delay between the pump and the seed pulses was controlled by a motorized linear translation stage, which was placed in the optical path of the seed beam. The seed and pump pulses were collinearly combined using a dichroic mirror and then were focused by an $f = 15$ cm planoconvex lens into the gas chamber filled with high-purity nitrogen gas. To minimize the seed produced by nonlinear propagation of the pump pulses (e.g., white-light or harmonic generations), we chose a relatively low gas pressure (i.e., 70 mbar) in all measurements. In particular, the external seed was polarized perpendicular to the polarization of the pump laser at all wavelengths; thus, the self-generated emission by the pump laser could be easily removed using a Glan-Taylor prism placed in front of the spectrometer. The output signal was then focused into a slit and completely captured by a grating spectrometer (Shamrock 303i, Andor), whereas the residual pump laser was removed using a stack of bandpass filters.

Figure 1(a) shows the forward spectrum of the external seed injected into the plasma channel generated by the 800-nm pump pulse with an optimized delay (blue dashed line). For comparison, the spectrum of the initial seed pulse is also presented (red solid line). Clearly, in the presence of the 800-nm pump pulse, a narrow-bandwidth peak with a central wavelength at ~391 nm appears on top of the spectrum of the seed pulse, which corresponds to the transition of $N_2^+(B^2\Sigma_u^+, v' = 0) \rightarrow N_2^+(X^2\Sigma_g^+, v = 0)$. The strong narrow-bandwidth 391-nm emission is ascribed to a seed-amplified N_2^+ laser owing to the population inversion between the $N_2^+(B^2\Sigma_u^+, v' = 0)$ and $N_2^+(X^2\Sigma_g^+, v = 0)$ states. We stress here that the two spectra in Fig. 1(a) are recorded by collecting all the photons in the signal beams into the spectrometer, which provides unambiguous evidence of the gain of the external seed during its propagation in the plasma channel. The observation clearly suggests that at the 800-nm pump wavelength, population inversion has occurred in the tunnel-ionized nitrogen molecules.

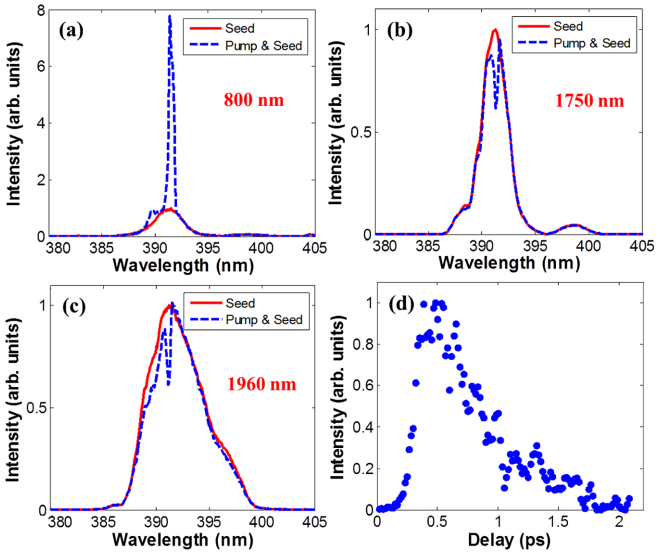

FIG. 1. (a) The forward spectra obtained by injecting an external seed pulse into the plasma channel induced by (a) 800-nm, (b) 1750-nm, and (c) 1960-nm pump pulses (blue dashed lines). For comparison, the spectra of the seed pulses are indicated by red solid lines in panels (a)–(c). (d) The temporal evolution of the 391-nm coherent emission with a time delay between the pump and seed pulses at the pump wavelength of 800 nm.

Next, we performed the same measurement using the wavelength-tunable midinfrared pump pulses from the OPA. At multiple pump wavelengths ranging from 1200 to 2000 nm, the experimental results are similar, as shown by the typical spectra recorded at pump wavelengths of 1750 and 1960 nm in Figs. 1(b) and 1(c). At the pump wavelength of 1750 nm, neither the third nor the fifth harmonics cover the frequency of the transition of $N_2^+(B^2\Sigma_u^+, v'=0) \rightarrow N_2^+(X^2\Sigma_g^+, v=0)$. In contrast, the fifth harmonic of the 1960-nm pump laser covers the transition wavelength of ~391 nm, which offers a self-generated seed source. To focus on the influence of the pump wavelength, we managed to maintain the same experimental parameters (e.g., pump energy, focusing geometry, gas pressure, seed wavelength, seed energy, etc.) as those in Fig. 1(a). Interestingly, as compared to the result obtained with the 800-nm pump pulses, the spectra of the external seed pulses show a significant absorption peak at ~391 nm when the pump wavelengths are set at 1750 and 1960 nm, as illustrated in Figs. 1(b) and 1(c), respectively. This observation indicates that more ions are populated at the

ground $N_2^+(X^2\Sigma_g^+, v=0)$ state as compared to the excited $N_2^+(B^2\Sigma_u^+, v'=0)$ state, and, thus, no population inversion is built up at the two pump wavelengths. The comparison shows that the population inversion responsible for the 391-nm N_2^+ laser has a strong dependence on the pump wavelength.

It is noteworthy that the narrow-bandwidth laserlike emission at ~391 nm has previously been observed without the injection of the external seed at the pump wavelengths in Figs. 1(a)–1(c). The origin of the emission obtained with the midinfrared pump sources is yet to be identified; this will be a subject of future investigation. Below, we will focus our attention on the mechanism behind the population inversion generated at the 800-nm pump wavelength. Specifically, we have measured the gain dynamics of the 391-nm emission as a function of the time delay between the pump and the seed pulses, as shown in Fig. 1(d). It was found that the gain increases rapidly on a time scale of ~300 fs followed by a relatively slow decay on the time scale of ~1 ps, which is consistent with our previous measurement [24].

To gain further insight into the underlying mechanism of the experimental observations, we perform time-dependent quantum-wave-packet calculations to simulate the dynamic processes of nitrogen molecular ions in strong laser fields. Because the tunneling ionization rate exponentially depends on the laser electric field, the ionization always occurs near the peak of the pump laser pulses. Ionizations from different molecular orbitals generate molecular nitrogen ions in different electronic states, the vibrational populations of which are determined by the Franck-Condon transition from neutral nitrogen molecules to molecular nitrogen ions in the corresponding electronic states [25]. In addition to the direct ionization from lower-lying orbitals [26], electronically excited molecular ions can also be generated from the ground electronic state through collision with the rescattering electron [27] or through photon absorption via single or multiphoton processes [28,29]. For simplicity, we assume that 20% of molecular nitrogen ions populate in the $A^2\Pi_u$ state and 20% populate in the $B^2\Sigma_u^+$ state. After the generation of nitrogen molecular ions, the remaining laser field will cause the coupling of the electronic states and promote the population exchanges among them. The time-dependent Schrödinger equation for describing the couplings among these electronic states is given by

$$i\frac{\partial}{\partial t}\begin{pmatrix}\Psi_X(R,t)\\ \Psi_A(R,t)\\ \Psi_B(R,t)\end{pmatrix} = \left[-\frac{1}{2\mu}\frac{\partial^2}{\partial R^2} + V(R,t)\right]\begin{pmatrix}\Psi_X(R,t)\\ \Psi_A(R,t)\\ \Psi_B(R,t)\end{pmatrix}, \quad (1)$$

where atomic units are used, μ is the reduced mass, and R is the internuclear separation of N_2^+. The potential matrix $V(R,t)$ for the three-state system can be written as

$$V(R,t) = \begin{pmatrix} V_X(R) & \vec{\mu}_{XA}(R)\cdot\vec{E}(t) & \vec{\mu}_{XB}(R)\cdot\vec{E}(t)\\ \vec{\mu}_{XA}(R)\cdot\vec{E}(t) & V_A(R) & 0\\ \vec{\mu}_{XB}(R)\cdot\vec{E}(t) & 0 & V_B(R)\end{pmatrix}, \quad (2)$$

where the diagonal elements denote, respectively, the Born-Oppenheimer potential energy curves (PECs) of $N_2^+(X^2\Sigma_g^+)$, $N_2^+(A^2\Pi_u)$ and $N_2^+(B^2\Sigma_u^+)$. The off-diagonal elements denote the coupling terms induced by laser fields under dipole approximation, with $\vec{\mu}_{XA}(R)$ and $\vec{\mu}_{XB}(R)$ being the electronic transition moments (TMs) between the relevant pairs of electronic states. $\vec{E}(t)$ represents the linearly polarized laser field with a constant amplitude for the first three optical cycles and a Gaussian falling edge of 12 cycles. The laser frequency and peak intensity (i.e., 2.2×10^{14} W/cm^2) are taken to be the same as the experimental parameters. Because the photoionization occurs predominantly near the peak of the pump laser pulse, it is reasonable to choose this laser profile when the strong field-induced population transfer is calculated.

Using the MOLPRO package [30], we perform state-of-the-art *ab initio* calculations for PECs and TMs. The details of the theoretical calculation can be found in the Supplemental Material [31]. Figure 2(a) shows the PECs of $N_2^+(X^2\Sigma_g^+)$, $N_2^+(A^2\Pi_u)$, $N_2^+(B^2\Sigma_u^+)$, and $N_2(X^1\Sigma_g^+)$. It should be noted that $\vec{\mu}_{XA}(R)$ is perpendicular to the molecular axis and $\vec{\mu}_{XB}(R)$ is parallel to the molecular axis. There is no dipole moment between the $N_2^+(A^2\Pi_u)$ and $N_2^+(B^2\Sigma_u^+)$ states. In the simulation, we included all the possible orientations of the molecular axis and averaged them with angular-dependent ion yields. As shown in Fig. 2(b), efficient population exchanges are observed between the ground and the two excited electronic states at the 800-nm pump wavelength. The population mainly distributes in the ground electronic state of N_2^+ immediately after the ionization. The remaining laser fields cause the population transfer between the ground and the excited electronic states. At the end of the laser pulse, the population in the $N_2^+(A^2\Pi_u)$ state is greatly increased, while that in the $N_2^+(X^2\Sigma_g^+)$ state is greatly decreased. As a result, the final population in $N_2^+(B^2\Sigma_u^+)$ becomes higher than that in $N_2^+(X^2\Sigma_g^+)$. We further explore the vibrational distribution of each electronic state of N_2^+ by projecting the final wave packets onto the field-free vibrational eigenfunctions. Figure 2(c) shows the vibrational distribution of $N_2^+(B^2\Sigma_u^+)$. It can be seen that the excited ions are mainly populated in the ground vibrational state. The results demonstrate that the population inversion has been formed between the $N_2^+(B^2\Sigma_u^+, v'=0)$ and $N_2^+(X^2\Sigma_g^+, v=0)$ states. The population inversion leads to the amplification of the seed pulse at ~391 nm, which agrees with our experimental observation in strong laser fields of 800-nm

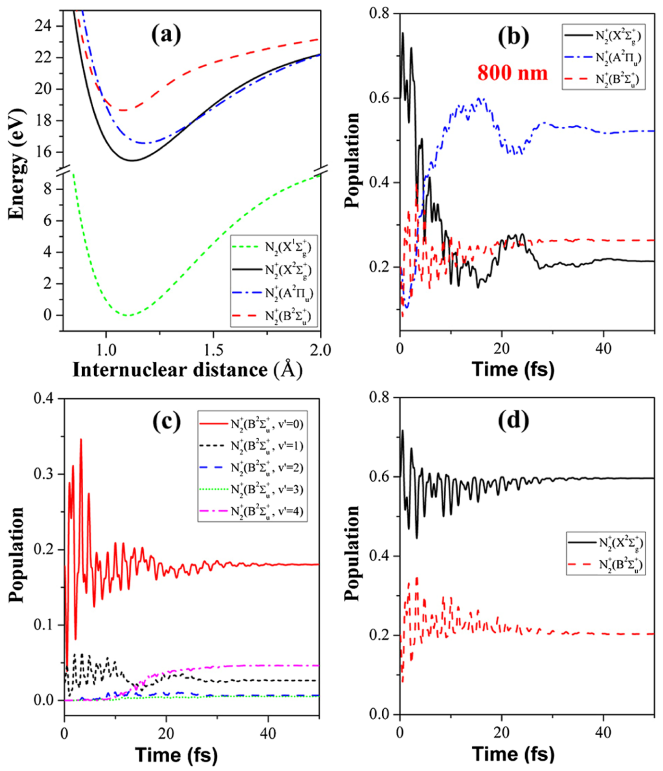

FIG. 2. (a) Potential energy curves of the electronic states obtained by cubic spline interpolation of *ab initio* data using the MOLPRO package. (b) The temporal evolution of the population distributions in the electronic states of N_2^+ in the 800-nm laser field with an intensity of 2.2×10^{14} W/cm^2. (c) The temporal evolution of vibrational states distribution of $N_2^+(B^2\Sigma_u^+)$ in the 800-nm laser field. (d) The temporal evolution of the population distributions in the $N_2^+(X^2\Sigma_g^+)$ and $N_2^+(B^2\Sigma_u^+)$ states obtained by removing the $N_2^+(A^2\Pi_u)$ states.

wavelength. Last but not least, it should be noted that although there is no direct coupling between the $N_2^+(A^2\Pi_u)$ and $N_2^+(B^2\Sigma_u^+)$ states, the participation of the $N_2^+(A^2\Pi_u)$ state is indispensable for generating the observed population inversion between the excited $N_2^+(B^2\Sigma_u^+)$ state and the ground $N_2^+(X^2\Sigma_g^+)$ state. As evidenced by Fig. 2(d), if we remove the coupling between the $N_2^+(A^2\Pi_u)$ and $N_2^+(X^2\Sigma_g^+)$ states, the molecular ions will be dominantly populated in $N_2^+(X^2\Sigma_g^+)$ but not $N_2^+(B^2\Sigma_u^+)$ state.

In our simulations, we also found that generating the population inversion strongly relies on the pump wavelength. As shown in Figs. 3(a) and 3(b), the couplings between the ground state and the excited electronic states are very weak when the pump wavelengths are 1750 and 1960 nm, and population inversion remains unachieved. In fact, our simulations show that at the peak intensity and pulse duration shown in Fig. 2(b), population inversion cannot be achieved with pump wavelengths in the 1200–2000 nm range. This also agrees with our experimental results.

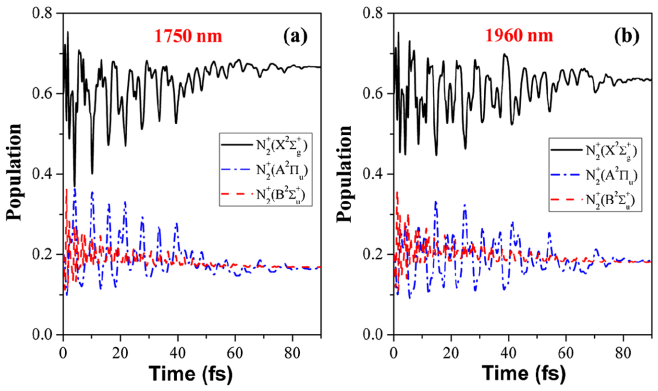

FIG. 3. The temporal evolution of the population distributions calculated at the pump wavelengths of (a) 1750 nm and (b) 1960 nm.

To further reveal the physical origin behind the observation of population inversion, we calculated the motion of nuclear wave packets and the time evolution of vibrational distribution in the strong laser fields. The detailed wave packet analysis can be found in the Supplemental Material [31–34]. Based on theoretical calculations and our experimental observations, we provide the following physical picture of the generation of population inversion in the tunnel-ionized nitrogen molecules in strong laser fields. As illustrated in Fig. 4(a), most nitrogen molecules remain neutral in the rising edge of the pump laser field; this is

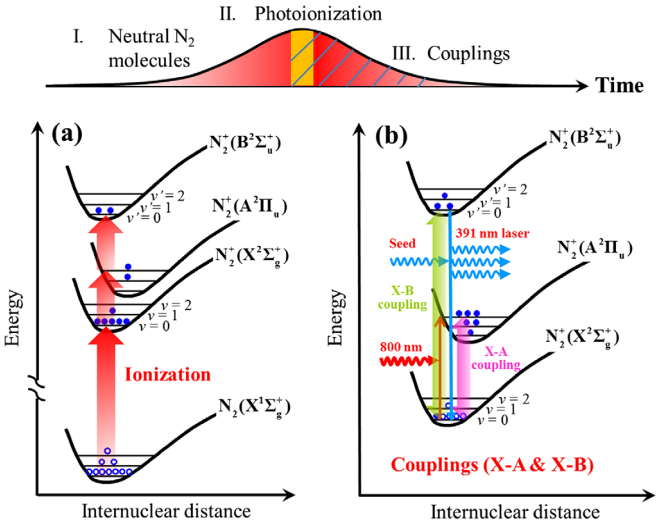

FIG. 4. Schematic diagram of the pumping mechanism for establishing population inversion in the 800-nm laser field. In region I of the pump pulse, photoionization is weak and most molecules remain neutral. (a) Near the peak of envelope of the driver laser, the molecules are populated to various electronic states of N_2^+ by tunnel ionization (region II, orange area). (b) After tunnel ionization, populations are redistributed among the three electronic states of N_2^+ through efficient couplings between the ground and the excited states (region III, hatched area of the pump pulse).

because tunnel ionization is highly sensitive to the field strength. When approaching the peak of envelope of the driver laser, the molecules are rapidly ionized and populated to various electronic states. According to the laser parameters of our experiment, the molecular nitrogen ions are mainly distributed in the ground vibrational state of $N_2^+(X^2\Sigma_g^+)$. After the generation of molecular nitrogen ions, as shown in Fig. 4(b), population transfers occur between the ground and the two excited electronic states due to the couplings induced by the strong laser field [35]. As a result, most $N_2^+(X^2\Sigma_g^+)$ ions are transferred to $N_2^+(A^2\Pi_u)$ through one-photon, near-resonant coherent excitation, which helps to establish the population inversion between $N_2^+(X^2\Sigma_g^+)$ and $N_2^+(B^2\Sigma_u^+)$ in the 800-nm laser field. Obviously, the participation of the $N_2^+(A^2\Pi_u)$ state serves as a reservoir for evacuating the population in the $N_2^+(X^2\Sigma_g^+)$ state and is indispensable for generating the population inversion between the excited $N_2^+(B^2\Sigma_u^+)$ state and the ground $N_2^+(X^2\Sigma_g^+)$ state. Furthermore, our theoretical simulations show that population inversion can be achieved for a broad range of the laser parameters (see Fig. S4 in the Supplemental Material [31]), which is consistent with the large number of experimental observations that have been so far reported on the strong-field-induced N_2^+ laser [16,17,21].

To conclude, we have performed experimental and theoretical investigations on the populations of tunnel-ionized nitrogen molecules with strong laser fields. It is generally known that tunnel ionization from lower-lying orbitals can lead to the direct generation of molecular nitrogen ions in excited states, but their populations are much less than in the ground state. Including the photoelectron recollision and photon absorption can greatly promote the excitation efficiency, whereas the populations in the excited states are still too low to accomplish the population inversion required for initiating any lasing actions. However, due to the couplings of the ground and excited states induced by the strong laser fields, efficient population exchanges between the ground and excited electronic states occur; these play a crucial role in the generation of both spontaneous fluorescence and laser emissions from the molecular nitrogen ions. Our findings not only unlock the puzzle of the strong-field-induced air lasing in tunnel-ionized nitrogen molecules, but also have important implications for investigating the excited-state dynamics of molecular ions in intense laser fields.

The authors would like to thank Dr. Aijie Zhang for her assistance on the *ab initio* calculations. This work is supported by the National Basic Research Program of China (Grants No. 2013CB922403 and No. 2014CB921303), and the National Natural Science Foundation of China (Grants No. 11134010, No. 61590934, No. 21373113, No. 11474009, No. 11434002, No. 61575211, No. 11304330, and No. 11404357).

*cywu@pku.edu.cn
†rflu@njust.edu.cn
§ya.cheng@siom.ac.cn

[1] L. V. Keldysh, Zh. Eksp. Teor. Fiz. **47**, 1945 (1964) [Sov. Phys. JETP **20**, 1307 (1965)].
[2] H. Niikura, F. Légaré, R. Hasbani, M. Y. Ivanov, D. M. Villeneuve, and P. B. Corkum, Nature (London) **421**, 826 (2003).
[3] X. M. Tong, Z. X. Zhao, and C. D. Lin, Phys. Rev. Lett. **91**, 233203 (2003).
[4] J. Hu, K. L. Han, and G. Z. He, Phys. Rev. Lett. **95**, 123001 (2005).
[5] M. Meckel, D. Comtois, D. Zeidler, A. Staudte, D. Pavičić, H. C. Bandulet, H. Pépin, J. C. Kieffer, R. Dörner, D. M. Villeneuve, and P. B. Corkum, Science **320**, 1478 (2008).
[6] C. I. Blaga, J. Xu, A. D. DiChiara, E. Sistrunk, K. Zhang, P. Agostini, T. A. Miller, L. F. DiMauro, and C. D. Lin, Nature (London) **483**, 194 (2012).
[7] X. M. Tong, Z. X. Zhao, and C. D. Lin, Phys. Rev. A **66**, 033402 (2002).
[8] D. Pavičić, K. F. Lee, D. M. Rayner, P. B. Corkum, and D. M. Villeneuve, Phys. Rev. Lett. **98**, 243001 (2007).
[9] B. K. McFarland, J. P. Farrell, P. H. Bucksbaum, and M. Gühr, Science **322**, 1232 (2008).
[10] O. Smirnova, Y. Mairesse, S. Patchkovskii, N. Dudovich, D. Villeneuve, P. Corkum, and M. Y. Ivanov, Nature (London) **460**, 972 (2009).
[11] H. Akagi, T. Otobe, A. Staudte, A. Shiner, F. Turner, R. Dörner, D. M. Villeneuve, and P. B. Corkum, Science **325**, 1364 (2009).
[12] I. Znakovskaya, P. von den Hoff, S. Zherebtsov, A. Wirth, O. Herrwerth, M. J. J. Vrakking, R. de Vivie-Riedle, and M. F. Kling, Phys. Rev. Lett. **103**, 103002 (2009).
[13] C. Wu, H. Zhang, H. Yang, Q. Gong, D. Song, and H. Su, Phys. Rev. A **83**, 033410 (2011).
[14] J. Wu, L. Ph, H. Schmidt, M. Kunitski, M. Meckel, S. Voss, H. Sann, H. Kim, T. Jahnke, A. Czasch, and R. Dörner, Phys. Rev. Lett. **108**, 183001 (2012).
[15] J. Yao, G. Li, X. Jia, X. Hao, B. Zeng, C. Jing, W. Chu, J. Ni, H. Zhang, H. Xie, C. Zhang, Z. Zhao, J. Chen, X. Liu, Y. Cheng, and Z. Xu, Phys. Rev. Lett. **111**, 133001 (2013).
[16] J. Yao, G. Li, C. Jing, B. Zeng, W. Chu, J. Ni, H. Zhang, H. Xie, C. Zhang, H. Li, H. Xu, S. L. Chin, Y. Cheng, and Z. Xu, New J. Phys. **15**, 023046 (2013).
[17] Q. Luo, W. Liu, and S. L. Chin, Appl. Phys. B **76**, 337 (2003).
[18] P. R. Hemmer, R. B. Miles, P. Polynkin, T. Siebert, A. V. Sokolov, P. Sprangle, and M. O. Scully, Proc. Natl. Acad. Sci. U.S.A. **108**, 3130 (2011).
[19] J. Yao, B. Zeng, H. Xu, G. Li, W. Chu, J. Ni, H. Zhang, S. L. Chin, Y. Cheng, and Z. Xu, Phys. Rev. A **84**, 051802(R) (2011).
[20] D. Kartashov, S. Alisauskas, A. Pugzlys, M. N. Shneider, and A. Baltuska, J. Phys. B **48**, 094016 (2015).
[21] G. Point, Y. Liu, Y. Brelet, S. Mitryukovskiy, P. Ding, A. Houard, and A. Mysyrowicz, Opt. Lett. **39**, 1725 (2014).
[22] M. Lezius, V. Blanchet, D. M. Rayner, D. M. Villeneuve, A. Stolow, and M. Y. Ivanov, Phys. Rev. Lett. **86**, 51 (2001).
[23] Z. B. Walters and O. Smirnova, J. Phys. B **43**, 161002 (2010).

[24] H. Zhang, C. Jing, J. Yao, G. Li, B. Zeng, W. Chu, J. Ni, H. Xie, H. Xu, S. L. Chin, K. Yamanouchi, Y. Cheng, and Z. Xu, Phys. Rev. X **3**, 041009 (2013).
[25] A. Becker, A. D. Bandrauk, and S. L. Chin, Chem. Phys. Lett. **343**, 345 (2001).
[26] S. Petretti, Y. V. Vanne, A. Saenz, A. Castro, and P. Decleva, Phys. Rev. Lett. **104**, 223001 (2010).
[27] Y. Liu, P. Ding, G. Lambert, A. Houard, V. Tikhonchuk, and A. Mysyrowicz, Phys. Rev. Lett. **115**, 133203 (2015).
[28] B. D. Esry, A. M. Sayler, P. Q. Wang, K. D. Carnes, and I. Ben-Itzhak, Phys. Rev. Lett. **97**, 013003 (2006).
[29] I. V. Litvinyuk, A. S. Alnaser, D. Comtois, D. Ray, A. T. Hasan, J. C. Kieffer, and D. M. Villeneure, New J. Phys. **10**, 083011 (2008).
[30] H.-J. Werner, P. J. Knowles, R. Lindh, F. R. Manby, M. Schütz *et al.*, computer code MOLPRO, version 2006.1, 2006, http://www.molpro.net..
[31] See Supplemental Material at http://link.aps.org/supplemental/10.1103/PhysRevLett.116.143007, which includes Refs. [16,17,21,26–30,32–34], for the details of theoretical simulation.
[32] S. R. Langhoff, C. W. Bauschlicher, Jr., and H. Partridge, J. Chem. Phys. **87**, 4716 (1987).
[33] S. R. Langhoff and C. W. Bauschlicher, Jr., J. Chem. Phys. **88**, 329 (1988).
[34] R. F. Lu, P. Y. Zhang and K. L. Han, Phys. Rev. E **77**, 066701 (2008).
[35] H. Metiu and V. Engel, J. Opt. Soc. Am. B **7**, 1709 (1990).